



Electrocatalytic and corrosion behaviour of tungsten carbide in near-neutral pH electrolytes

Falk Harnisch, Uwe Schröder*, Marion Quaas, Fritz Scholz

Institute of Biochemistry, University of Greifswald, Felix-Hausdorff-Strasse 4, 17487 Greifswald, Germany

ARTICLE INFO

Article history:

Received 20 June 2008

Received in revised form 4 August 2008

Accepted 17 August 2008

Available online 26 August 2008

Keywords:

Tungsten carbide

WC

Electrocatalysis

Microbial fuel cell

Corrosion

Biofuel cell

ABSTRACT

This paper examines the electrochemical and electrocatalytic behaviour of tungsten carbide at ambient temperature and at near to neutral pH conditions. The electrocatalytic oxidation of hydrogen, formate and lactate is investigated as a function of the composition of the catalyst material, and of the composition and pH of the used electrolyte solutions. It is demonstrated that for the oxidation of hydrogen, different surface and bulk properties are decisive than for the oxidation of formate and lactate. A major problem of tungsten carbide is its stability in aqueous, pH neutral environments, in which noticeable corrosion processes take place. The individual corrosion rates strongly depend on the electrolyte composition and pH, and on the presence of reducing agents.

© 2008 Elsevier B.V. All rights reserved.

1. Introduction

Tungsten carbide, WC, is a fascinating and at the same time contradictory material. On the one hand it has been a hope for the fuel cell community, on the other hand – based on the complexity of its bulk and surface properties and chemistry – it defies a simple examination and evaluation. Since the 1960s tungsten carbide (WC) has been considered as an anode material for hydrogen [1] or methanol fuel cells [2]. Although the performance of tungsten carbide may be inferior in direct comparison to platinum [2], its low price and its insensitivity to catalyst poisons like H₂S and CO [3] make it an interesting alternative to the noble metal catalyst. The low price and the insensitivity to catalyst poisons are properties that make tungsten carbide also a promising anode catalyst in primary metabolite based microbial fuel cells (MFCs) [4,5]. For this field of application, a further property of this catalyst—its ability to catalyze the oxidation of a variety of reduced primary microbial metabolites, such as hydrogen, formic acid and lactic acid is of great importance [6].

Although the first results of the use of WC as MFC catalyst are promising, they are only initial. Many issues remain to be addressed, and it can be expected that by tailoring the electrocatalyst properties (i.e., structural, physical and chemical bulk and

surface properties) a considerable improvement of the electrocatalytic behaviour and therefore of the microbial fuel cell performance can be achieved.

The electrochemical behaviour of tungsten carbide is strongly dependent on its surface composition and condition. Thus, for example, the carbon content of the surface layers is decisive for the electrocatalytic performance of the material: Whereas carbon deficiencies support the electrocatalysis, the presence of (pre)graphitic carbon at the particle surface has been reported to suppress the electrocatalytic activity [7–9].

Most significant for the electrocatalysis at tungsten carbide is the presence of oxygen species (tungsten oxides) at the catalyst surface. The formation, the composition and the stability of these oxides are of utmost importance for the electrochemical and electrocatalytic behaviour and for the stability of tungsten carbide in aqueous environments. Since, in turn, the chemistry of these oxides will depend on the nature and the pH of the aqueous electrolytes, these solution properties can be expected to have a great influence on the properties of tungsten carbide.

This paper examines the electrochemical and electrocatalytic behaviour of tungsten carbide from the viewpoint of an application as an anode catalyst in microbial fuel cells. Emphasis is put on the investigation of the electrocatalytic oxidation of hydrogen, formate and lactate – major products of microbial fermentation processes – as a function of the composition of the catalyst material, and of the composition and pH of the used electrolyte solutions.

* Corresponding author. Tel.: +49 3834 864330; fax: +49 3834 864451.

E-mail address: uweschr@uni-greifswald.de (U. Schröder).

For a better understanding of the experimental results of this study, and of the complex properties of tungsten carbide in general, a literature section precedes the paper, summarizing the present knowledge of the material with respect to the subjects of discussion.

2. Literature survey

2.1. Basic chemical properties and redox behaviour of tungsten carbide

Tungsten carbide belongs to a group of materials known as interstitial alloys of group IV B–VI B transition metals, in which elements like carbon (or nitrogen, silicon or phosphorus) atoms occupy the interstitial lattice positions of the metal [10,11]. These materials possess properties known from the group VIII metals, like of the precious metals platinum or palladium [12]. Thus, they show remarkable catalytic activities, which have been attributed to a distinct electronic structure induced by the presence of carbon, nitrogen or of phosphorus in the metal lattice [13]. In the case of tungsten carbide, its catalytic activity has been explained by the filling of the d-states at the Fermi level of tungsten by the alloying carbon [14,15].

Yet, although tungsten carbide has by some authors been discussed to be isoelectronic to platinum [12] it does not share its inertness. When exposed to air, surface oxidation takes place and advances with time [16]. Generally one can assume that tungsten carbide is, if not stored under inert gas atmosphere, always covered by oxidic species [17]. When exposed to water, tungsten carbide undergoes continuous oxidation and dissolution. This process is pH dependent and follows zero-order kinetics [17]. In an earlier work, Voorhies [18] already pointed out that the standard Gibbs free energy ΔG^0 of the WC oxidation is $-1336 \text{ kJ mol}^{-1}$, which leads to the conclusion that oxidants with a formal potential more positive than +100 mV (vs. SHE) will oxidise the surface of WC particles. This was also shown by Human and Exner [19] who estimated the corrosion potential of WC in N_2 purged 0.1N H_2SO_4 to be -105 mV (vs. Ag/AgCl). When the tungsten carbide particle is covered by an insulating layer of WO_3 no further oxidation will take place until a higher oxidation potential ($>1 \text{ V}$ vs. SHE) is applied, that leads to the complete oxidation of the particle [20]. This result was also confirmed for the chemical oxidation of WC. Thus, it has been demonstrated that mild oxidants like ferricyanide ($E^0 = 0.69 \text{ V}$ vs. SHE) lead to an oxide monolayer formation, whereas stronger oxidants like Ce^{4+} ($E^0 = 1.46 \text{ V}$ vs. SHE) lead to bulk oxidation [18].

At ultra high vacuum deposited tungsten carbide the film's exact composition has been shown to critically influence its stability: whereas W_2C was readily oxidized in 0.5 M H_2SO_4 at 500 mV (vs. NHE), WC was stable up to the oxygen evolution potential [21,22].

The surface oxidation of tungsten carbide preferentially progresses on sites, where oxidic species already exist [23]. It leads to a simultaneous oxidation of tungsten and carbon. Carbon is oxidized to CO_2 , e.g., visible as a gas formation when tungsten carbide electrodes are oxidatively polarized (see, e.g. [7]). The exact nature of the formed tungsten oxides is difficult to characterize and is strongly depending on the applied potential, electrolyte composition, particle geometry and particle pre-treatment. This relatively undefined composition of the surface oxide layers may be the major reason for the varying rest potentials of tungsten carbide electrodes, immersed in similar electrolyte solutions [23]. They also explain the irreproducible hydrogen adsorption potentials at tungsten carbide [23,24].

2.2. Electrocatalytic hydrogen oxidation at WC

The catalytic activity of tungsten carbide depends on many parameters. A major factor is the atomic ratio of tungsten and carbon [8] in the interstitial alloy. Thus, it is commonly acknowledged that high catalytic activity requires a carbon deficiency in the material [25,16]. Other factors like the particle size, e.g., [26], lattice defects [26] and pseudometallic surfaces [9] have been (often controversially) discussed. Yet, one of the major factors that have been discussed to be determining for the electrocatalytic behaviour is the presence of oxidic species at the WC surface. Already in 1970 Böhm demonstrated that on freshly prepared WC electrodes with low oxide surface coverage no appreciable hydrogen adsorption takes place [27]. Only after anodic polarization the hydrogen adsorption properties could be improved, which was explained by the facilitated hydrogen adsorption at the formed surface oxide species. This activation of the hydrogen adsorption (and consequently of the rate of hydrogen oxidation) by anodic polarization has been discussed by various authors. It has been shown that the electrochemical or chemical activation (oxidation) in electrolyte solutions leads to similar surface oxide layers as an extended exposure to humid air [16].

The effect of activation can be reversed by an exposure of the WC sample to high temperatures in an inert gas atmosphere [7] or in hydrogen [9], a procedure that reduces the surface species and removes oxygen from the WC particle surface. The activation leads to the oxidation of tungsten up to W(VI) , i.e., WO_3 . The thickness of the tungsten oxide surface layer, formed by anodic polarization, was found to be between two and three monolayers, with the predominant species being hydrated and non-hydrated WO_3 [7,9,23]. This oxide is known to be readily soluble in alkaline solutions as WO_4^{2-} . Therefore the anodic activation will here lead to a continuous dissolution of WC. At low pH, WO_3 is considered to be poorly soluble. Yet, due to its insulating properties it can inhibit any electrocatalytic activity. To prevent the inhibition, the addition of H_2 or hydrazine during the anodic activation has been proposed, e.g., [28]. The addition of the reducing agents leads to a partial reduction of WO_3 and the subsequent dissolution of the more water soluble WO_{3-x} species [29]. It is obvious that such procedure leads to an inevitable dissolution of the WC catalyst. Furthermore, the stability of WO_3 in acidic electrolyte solutions is rather questionable. The given proofs for the insolubility of WO_3 in acidic solutions originate from older literature, e.g., [28], and they are likely based on insufficient detection limits at that time. Newer publication clearly show that WO_3 layers on WC are not perfectly stable in 0.1 M H_2SO_4 when polarized to 0.7 V (vs. SCE) [22,30].

It has been demonstrated by different authors, that the activated electrodes lose their activity over time, however, levelling at an activity higher than that prior to the activation [31]. The authors conclude that at that stationary level, which is characterized only by a minimum activity loss, a continuous oxidation and dissolution of WC takes place. The rate of the dissolution process depends on several factors (apart from the electrolyte pH). Thus, the addition of cobalt ions has been shown to slow down the dissolution [20,32]. On the other hand, the presence of phosphate ions can greatly enhance the rate of dissolution—through the formation of soluble heteropolytungstates [6,33].

Taking into account that the activation procedure involves the formation of surface oxides, it is very likely that these oxides play the major role for the catalytic activity of tungsten carbide. Yet, this role has been discussed rather controversially. Whereas some authors speculated, that tungsten oxides are the catalytic centres, their ability to act as catalytic centres was denied in other studies [26]. But due to their complex nature and the individually proceeding oxidation process at the individual WC particle it is

hard to define the actual catalytic active site. Other authors also discussed, that the W(0), that forms during the oxidation of the WC surface is the actual reaction site [16].

2.3. Electrocatalytic oxidation of organic fuels

Already in the 1960th the electrocatalytic oxidation of organic compounds such as aldehydes and formic acid at tungsten carbide has been reported [34]. Further, the catalytic activity of several transition metal carbides, including WC, for the oxidation of methanol has been demonstrated, e.g., [35–39].

On the oxidation of these organic fuels at tungsten carbide, much less information is available than for hydrogen oxidation. Most information is related to the oxidation of methanol and formic acid. The oxidation of methanol appears to require both, high oxidation potentials (>0.4 V vs. SHE) and elevated temperatures (>50 °C)—both conditions are not suitable for microbial fuel cell applications. The oxidation of formic acid, too, requires elevated temperatures. Thus, Binder et al. reported – for a fixed current density of 0.5 mA cm^{-2} – an increase of the oxidation potential from 0 mV at 90 °C to 400 mV at 50 °C [34]. Further, depending on the current density, the oxidation of formic acid was reported to follow different mechanisms: at low current density, it proceeds via dehydrogenation and the subsequent oxidation of the formed hydrogen. This mechanism is accompanied by comparably low overpotentials (the oxidation takes place near the reversible hydrogen oxidation potential). The dehydrogenation appears to be rate limiting, so that the indirect oxidation is, at high current densities, replaced by a direct oxidation of the formic acid, a reaction that is accompanied by large overpotentials.

3. Experimental

3.1. WC-syntheses

All WC samples were synthesized from WO_3 (Strem Chemicals, Germany), which was dehydrated at 400 °C for at least 1 h in N_2 or Ar atmosphere. In the following step, the WO_3 powder was mixed with oxalic acid and NH_4Cl in a weight ratio of 4:2:1 [40]. The syntheses were performed at 800 °C and under CO atmosphere in a three-zone tube furnace (Carbolite, Germany). The CO-stream was generated by continuously dropping (flow rate $200 \mu\text{L min}^{-1}$) dry formic acid into concentrated H_2SO_4 using a peristaltic pump (ISMATEC, Germany). The CO-stream was passed over KOH or CaCO_3 to remove traces of water, CO_2 and formic acid.

After the carburization, the product was allowed to cool down to room temperature under argon or nitrogen atmosphere.

The basis for this study is a set of 40 catalyst samples, individually synthesized via the procedure described above. Table 1 provides an overview on basic parameters of these samples, such as composition and grain size as derived from X-ray powder analysis [6,9]. The analysis of the X-ray patterns reveals a relatively strong variation of the sample compositions. The major constituent of all samples is WC, however, most samples also contain various amounts of W and W_2C as side products of the reductive carburization and WO_2 , an indicator of an incomplete conversion of the reaction precursor. The deviating composition of the samples can most likely be attributed to the sensitivity of the reaction to variations in the flow rate of carbon monoxide and to small changes in the temperature distribution in the furnace. Although such deviation is usually disadvantageous for preparative procedures, it allows a systematic search for correlations between physical–chemical properties of the catalysts and its

Table 1

Grain size and chemical composition of the tungsten carbide samples, studied throughout this investigation

ID	Grain size WC (nm)	Fraction (%)			
		WC	W_2C	WO_2	W
IL_02	14.8	96.2	3.8	0.0	0.0
IL_03	11.1	96.8	3.2	0.0	0.0
IL_04	10.4	100.0	0.0	0.0	0.0
IL_05	30.4	34.5	54.8	10.7	0.0
IL_06	14.5	60.3	39.7	0.0	0.0
IL_07	11.8	100.0	0.0	0.0	0.0
IL_08	11.4	100.0	0.0	0.0	0.0
IL_09	12.1	100.0	0.0	0.0	0.0
IL_10	13.7	85.4	9.2	5.5	0.0
IL_10b	10.7	100.0	0.0	0.0	0.0
IL_11	11.4	100.0	0.0	0.0	0.0
IL_12	12.7	100.0	0.0	0.0	0.0
IL_19	14.9	100.0	0.0	0.0	0.0
IL_20	13.3	100.0	0.0	0.0	0.0
IL_21	12.1	96.6	3.4	0.0	0.0
IL_22	12.9	92.5	7.5	0.0	0.0
IL_23	12.0	100.0	0.0	0.0	0.0
IL_24	13.6	87.4	12.6	0.0	0.0
IL_25	12.8	94.8	5.2	0.0	0.0
IL_26	13.2	83.4	16.6	0.0	0.0
IL_27	13.4	89.5	3.3	7.2	0.0
IL_28	13.4	89.5	3.3	7.2	0.0
IL_29	14.2	61.5	38.5	0.0	0.0
IL_30	11.8	29.1	66.0	4.8	0.0
IL_31	15.9	74.9	25.1	0.0	0.0
IL_32	17.5	63.5	24.2	0.0	12.4
IL_33	12.9	95.6	0.0	0.0	4.4
IL_34	13.4	97.9	0.0	0.0	2.1
IL_35	13.1	93.5	3.7	0.0	2.8
IL_36	14.2	85.1	14.9	0.0	0.0
IL_37	18.8	52.4	47.6	0.0	0.0
IL_38v	16.5	13.1	85.0	1.8	0.0
IL_38h	3.0	6.2	47.0	46.8	0.0
IL_39	16.4	36.7	16.6	0.0	46.6
IL_40	16.7	40.3	8.3	0.0	51.3
IL_41	7.7	61.6	10.2	28.2	0.0
IL_42	7.4	42.8	13.7	43.5	0.0
IL_43a	6.5	75.0	9.3	15.7	0.0
IL_43b	5.9	68.2	12.2	19.6	0.0
IL_44	8.1	95.3	4.7	0.0	0.0
IL_45	15.6	78.1	21.9	0.0	0.0
IL_46	13.4	83.4	16.6	0.0	0.0
IL_47	17.3	17.6	15.0	0.0	67.4
IL_48	16.1	9.0	12.4	1.7	76.9

electrochemical and electrocatalytic behaviour and was for this reason chosen for this study.

3.2. Electrode preparation

As the electrode substratum, polycrystalline sintered graphite in the form of graphite discs (\varnothing 4.9 mm, 0.19 cm^2 geometrical surface area) was used. The polycrystalline graphite electrodes (for spectral analysis, Elektrokohle, Lichtenberg, Germany) were paraffin impregnated in order to prevent a soaking with electrolyte solutions [41].

For electrode preparation a defined amount of the tungsten carbide powder (~ 20 mg) was mixed with 5% Nafion[®] solution and hand-pressed onto the graphite disc. The electrodes were allowed to dry in air at ambient temperature and were then electrochemically characterized.

3.3. Electrochemical characterization

All electrochemical experiments were carried out using a conventional three electrode setup, with a platinum electrode as

the counter electrode and a silver/silver chloride (saturated KCl; 0.197 V vs. SHE) reference electrode. The experiments were performed using an Autolab PGSTAT 20 potentiostat/galvanostat (Ecochemie, The Netherlands) and a rotating disc electrode device (EG&G, USA).

For the determination of the electrocatalytic hydrogen oxidation activity, chronoamperometry (constant potential of 0.2 V vs. Ag/AgCl), cyclic voltammetry (scan rate of 2 mV s⁻¹) as well as galvanodynamic polarization (scan rate 0.01 μA s⁻¹) were carried out in nitrogen or hydrogen bubbled electrolyte solution. An electrode rotation rate of 1000 rpm was chosen based on preceding experiments, in order to avoid mass transfer limitation.

For measuring the catalytic activity towards the oxidation of formate and lactate, chronoamperometric measurements were carried out, at 0.2 V (vs. Ag/AgCl) and 1000 rpm electrode rotation rate.

Electrolyte solutions of 100 mM KCl, 100 mM H₂SO₄, 100 mM HCl and 100 mM sodium-phosphate-buffer at pH of 3, 7 and 10 served as electrolyte.

3.4. X-ray diffractometry

Composition and grain size of the catalyst powder were determined by X-ray diffraction. X-ray powder patterns were recorded using a HZG 4 Diffractometer (Seifert-FPM) in the Bragg-Brentano geometry. CuKα radiation (40 kV and 40 mA) was applied and an angle range from 15 to 90°/2θ was recorded at 0.02 increments and with 1 s counting time. The X-ray patterns were identified with the help of the PDF-2[®] X-ray database (International Centre for Diffraction Data, ICDD) referring to WC (#73-0471), hexagonal W₂C (#79-0743), W (#04-0806) and WO₂ (#86-0314). The mean grain size was determined using the Scherrer equation:

$$D = \frac{k \times \lambda}{\beta_{\text{corr}} \times \cos \theta};$$

with D is the grain size, k is the geometry factor, λ is the wave length of the elastic scattered radiation, β_{corr} is the full width at the half maximum (FWHM), corrected by an instrumental resolution width and θ the Bragg scattering angle.

In order to estimate the molar fractions of the major constituents in the catalyst samples the powder diffraction patterns of the samples were analysed with respect to the height of the most intensive reflections of identified compounds according to Vidick et al. [9]. For the evaluation of the resulting data it has to be taken into account this quantification represents only a rough approximation, since (i) the calculation relies on the peak heights rather than on the peak area and (ii) only the crystalline portions of the sample are measured.

3.5. ICP OES and ion chromatography

For the qualitative and quantitative determination of soluble tungsten species ion chromatography (IC) and inductively coupled plasma optical emission spectroscopy (ICP-OES) were used.

An ICS-1000 (Dionex, Germany) equipped with a Ion Pac AS9 HC column, ASRS-Ultra 4 mm electrochemical cation suppressor and a DS 6 heated conductivity cell was used for ion chromatography. The mobile phase was 12 mM Na₂CO₃ and 10 mM NaHCO₃.

The ICP OES was performed with an Optima 2100 series spectrometer (PerkinElmer, USA). The samples were diluted 1:10 before measurement and measured in 9 replicates. The standard deviation was always less than 5%.

4. Results and discussion

4.1. Electrocatalytic behaviour

Fig. 1 illustrates the electrocatalytic activity of a tungsten carbide modified electrode in 0.1 M KCl as a function of the applied potential. The figure clearly shows that the electrode has a distinct activity for the oxidation of hydrogen (A), formate (B) and lactate (C). With respect to the (biological) standard potentials of these substrates ($E^{\circ}_{\text{H}_2/2\text{H}^+} = -410 \text{ mV}$, $E^{\circ}_{\text{formate}/\text{CO}_2} = -432 \text{ mV}$, $E^{\circ}_{\text{lact.}/\text{pyruv.}} = -185 \text{ mV}$) the oxidation of formate proceeds at the highest, the oxidation of hydrogen with the lowest overpotential. An interesting feature of Fig. 1 is that the electrocatalytic oxidation of lactate and formate occurs at virtually identical potentials and at similar current densities (at comparable concentrations). Considering that the biological standard redox potentials of these compounds differ by about 250 mV, this finding indicates a common oxidation mechanism and rate-limiting step. The large overpotential of the oxidation of lactate and formate indicates the direct oxidation of these compounds rather than the indirect path, which would proceed at considerably lower overpotentials (see Section 2).

As stated in the literature part of this paper, the mechanisms and active sites for the oxidation of organic substrates such as formate at tungsten carbide may be different to those responsible for the oxidation of hydrogen [38]. But how much the mechanisms of the electrocatalytic oxidation and the nature of the involved active centres differ for hydrogen in comparison to the organic substrates is illustrated in Fig. 2. This figure reveals that samples that possess a high electrocatalytic activity for the oxidation of hydrogen possess a low activity for the oxidation of organic substrates like formate and lactate, and vice versa.

The reason for this peculiar behaviour, which has also been observed by other authors [42] can be derived from Fig. 3(A and B). These figures summarize the catalytic behaviour of the synthesized catalyst samples as a function of their composition (molar fractions of their constituents). They illustrate that the catalytic activities for the different target compounds depend on different catalyst constituents. Thus, the hydrogen oxidation activity correlates with the WC molar fraction of the samples. The

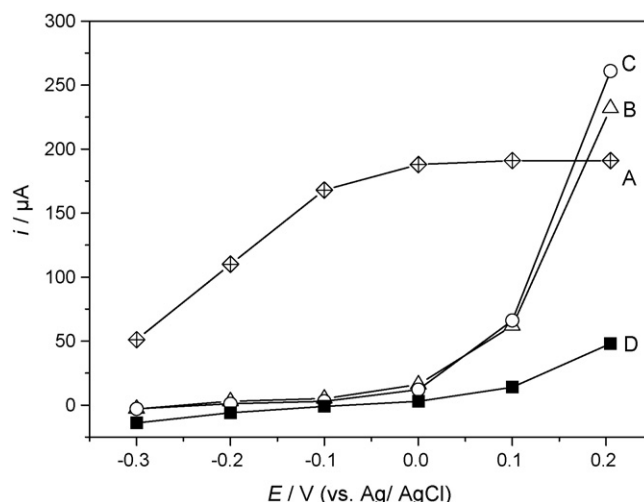


Fig. 1. Dependence of the stationary oxidation currents of (A) hydrogen, (B) formate (0.45 mol L⁻¹), and (C) lactate (0.45 mol L⁻¹) at WC, on the applied potential. The currents are derived from multi-step chronoamperometric experiments and have been corrected by subtracting the base current (D); electrolyte solution: 0.1 M KCl, pH 5.5; sample number: IL_41.

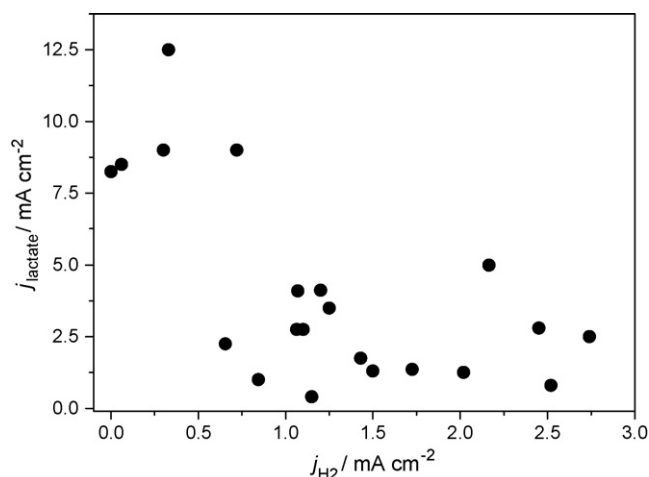


Fig. 2. Electrocatalytic current densities of different tungsten carbide samples for the oxidation of lactate, as a function of the hydrogen oxidation activity of the respective samples. Electrode potential: 0.2 V (vs. Ag/AgCl). Electrolyte solution: 0.1 M KCl, pH 5.5.

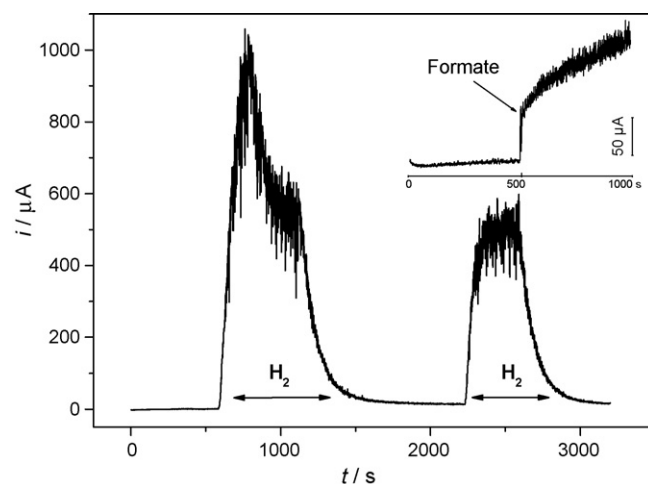


Fig. 4. Current vs. time plot of a WC modified electrode in 0.1 M KCl solution. The solution was intermittently purged with hydrogen and nitrogen. The electrode was stored in air prior to the experiment. Electrode potential: 0.2 V; sample number: IL_23.

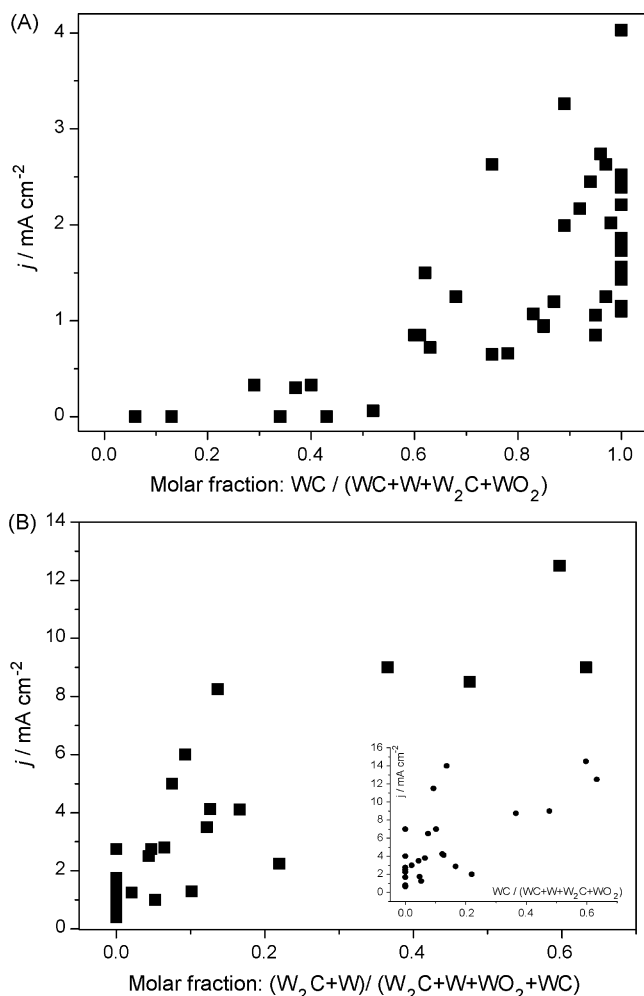


Fig. 3. Dependence of the electrocatalytic current densities of different catalyst samples on the sample composition, as derived from X-ray powder analysis. The currents are based on chronoamperometric experiments, performed at 0.2 V electrode potential; electrolyte solution: 0.1 M KCl, pH 5.5. (A) Electrocatalytic hydrogen oxidation; (B) main figure: oxidation of lactate, inset figure: oxidation of formate.

oxidation of the organic acids, on the other hand, relies on the presence of W_2C and W, side products of the carburization procedure. It is interesting to notice that the dependence of the catalytic currents on the molar fractions of W_2C or W alone (data not shown) show a much weaker correlation than that of the sum of both constituents (Fig. 3B) which indicates a synergetic effect, or the involvement of both species in the oxidation of the organic compounds.

Fig. 4 (main figure) illustrates an interesting phenomenon that occurs when WC modified electrodes that have been stored in humid air are used to oxidize hydrogen (in, e.g., hydrogen saturated KCl solution). The figure shows a strong decrease of the electrocatalytic activity during the first 500 s of hydrogen oxidation, from 5 mA cm^{-2} to reach a stable level 2.6 mA cm^{-2} . After interruption of the hydrogen supply for about 1000 s the current returned to this current density after the hydrogen supply was re-established. Only when the electrode was, for a longer period of time (more than 1 h), stored at air, the activity again reached the maximum level of 5 mA cm^{-2} . Such phenomenon is known as tungsten carbide activation. It is usually achieved by electrochemical polarization and oxidation (see Section 2), but as our results show, the storage of the catalyst in humid air already results in a similar effect. Raman measurements (data not shown) of our samples confirm the presence of surface oxides of these samples. But why does the activation last only so short time? The answer lies in the nature of the surface groups, formed during the activation procedure. As explained in Section 2, the activation is based on surface oxide formation and thus increased hydrogen adsorption behaviour of the catalyst. Yet, in neutral (or alkaline) environments these oxides possess a low stability, degradation taking place by dissolution in the electrolyte (formation of, e.g., WO_4^{2-}). Thus, in neutral and especially in alkaline solutions, oxides are quickly removed from the catalyst surface, and the activation effect vanishes.

The inset figure in Fig. 4 depicts that the surface oxidation of WC does not lead to an increased catalytic activity towards formate (or lactate; data not shown). Rather oppositely, the oxidation currents are low at the beginning and increase over time. This finding again emphasizes the involvement of very different species in the oxidation of hydrogen and organic compounds.

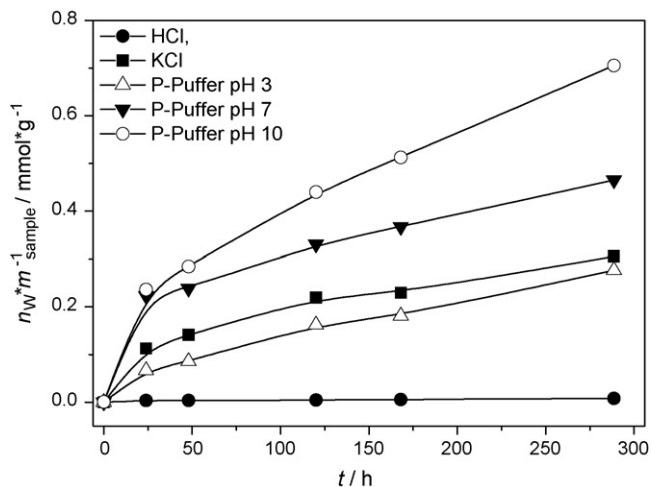


Fig. 5. Dissolution of WC powders in nitrogen purged, 0.1 M electrolyte solutions. About 22 mg catalyst were dispersed in 100 mL of the respective solution; the solutions were continuously stirred; sample number: II_12.

4.2. Chemically and electrochemically induced corrosion of tungsten carbide

As stated in Section 2 of this paper, tungsten carbide is readily oxidized by oxygen and other, even mild, oxidants. At low pH, this oxidation is confined to the catalyst surface, since the WO_3 layer protects the catalyst from further destruction. At alkaline pH, on the other hand, the solubility of WO_3 as WO_4^{2-} leads to a steady process of oxidation and dissolution, and thus to complete dissolution of the catalyst. But how sensitive tungsten carbide is against this oxidative dissolution even in the absence of obvious oxidants is shown in Fig. 5 (and in Table 2).

In this figure, the dissolution of tungsten carbide samples and the formation of soluble tungsten species in nitrogen purged electrolyte solutions, as a function of the electrolyte pH and composition is depicted. Figure shows that water itself can efficiently decompose tungsten carbide even at neutral pH. The rate of oxidation increases with increasing pH [17] and in the presence of phosphate ions. These effects are due to an increased solubility of tungsten oxides at higher pH values (formation of WO_4^{2-}) and the formation of heteropolytungstates. In 100 mM, pH 7 phosphate buffer solution, up to 6% of the material is dissolved after 24 h and 15% after 300 h.

Another undesired effect observed in our study is an increase of the rate of oxidative corrosion during the electrocatalytic oxidation of fuels at the catalyst. As shown in Fig. 6, the amount of tungsten released from the electrode into the nitrogen purged electrolyte solution (0–18 h) proceeds at a steady level of $0.08 \mu\text{mol h}^{-1}$. A correlation of the electric charge to the released tungsten yields 5.2 mol of electrons per mole tungsten, which is in good agreement

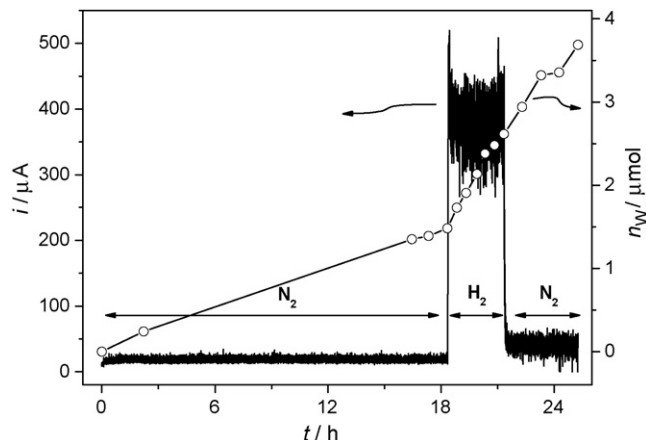


Fig. 6. Left axis: base current and catalytic current of a tungsten carbide modified electrode in nitrogen/hydrogen purged, 0.1 M KCl electrolyte solution. The potential of the working electrode was 0.2 V. Right axis: amount of WO_4^{2-} released into the electrolyte solution, as detected by ICP-OES during the electrochemical experiment; sample number: II_44.

with the assumption that $\text{W}(0)$ is oxidized to $\text{W}(\text{VI})$. With commencing hydrogen oxidation, the rate of dissolution increases by a factor of 4 and continues with a slightly decreased rate even after hydrogen supply was stopped. The background (corrosion) current of the electrode increased from $20 \mu\text{A}$ ($105 \mu\text{A cm}^{-2}$) prior to, to $40 \mu\text{A}$ ($210 \mu\text{A cm}^{-2}$) after hydrogen purging.

The increase of the corrosion current during hydrogen purging and hydrogen oxidation can be attributed to a partial reduction of the $\text{W}(\text{VI})$ surface oxides and the considerably higher solubility of these WO_{3-x} oxides in water compared to WO_3 . The continually high corrosion rate after the termination of the hydrogen supply is remarkable and difficult to explain. One reason may be an increase of the porosity (larger surface area) of the catalyst during the hydrogen oxidation.

5. Conclusions

In this publication, we have demonstrated the complexity of the electrochemical and electrocatalytic properties of tungsten carbide. We have shown that pure tungsten carbide, WC, may not be advantageous for microbial fuel cell application, since WC preferably oxidizes hydrogen—with low ability to oxidize organic metabolites such as formate and lactate. The additional presence of W and W_2C phases can improve the catalytic activity towards these compounds, and can thus improve the efficiency of the anodic metabolite oxidation. A problem to be solved is the liability of the catalyst to corrosion at pH neutral conditions, which leads to a slow but continuous dissolution of the catalyst.

For further investigations, additional information on surface properties, such as the exact surface composition (and possibly its change during catalyst operation), BET surface area and surface energy level will have to be gathered, in order to attain a deeper understanding of the processes and reaction mechanisms of tungsten carbide.

Acknowledgements

F.H. gratefully acknowledges Ph.D. scholarships by the Deutschen Bundesstiftung Umwelt (DBU) and the Studienstiftung des deutschen Volkes. U.S. acknowledges support by the Deutsche Forschungsgemeinschaft (Research grant and Heisenberg Program). We thank Iris Herrmann (Hahn–Meitner Institute, Berlin) for conducting the Raman spectroscopic experiments.

Table 2

Corrosion rates of a WC sample at 0.2 V (vs. Ag/AgCl) in different nitrogen purged electrolytes

Electrolyte 100 mM	Corrosion rate [$\text{mol}_\text{W} \text{ h}^{-1} \text{ cm}^{-2}$]
KCl	$\sim 4.5 \times 10^{-7}$
H_2SO_4	$\sim 3.6 \times 10^{-7}$
HCl	$\sim 2.2 \times 10^{-7}$
Phosphate buffer	
pH 3	$\sim 4.3 \times 10^{-7}$
pH 7	$\sim 3.8 \times 10^{-6}$
pH 10	$\sim 1.6 \times 10^{-5}$

References

- [1] H. Böhm, F.A. Pohl, Wiss. Ber. AEG-Telefunken 41 (1968) 46.
- [2] D. Baresel, W. Gellert, J. Heidemeyer, P. Scharner, Angew. Chem. Int. Ed. 10 (1971) 194.
- [3] V.S. Palanker, R.A. Gajyev, D.V. Sokolsky, Electrochim. Acta 22 (1977) 133.
- [4] U. Schröder, Phys. Chem. Chem. Phys. 9 (2007) 2619.
- [5] M. Rosenbaum, F. Zhao, U. Schröder, F. Scholz, Angew. Chem. Int. Ed. 45 (2006) 6658.
- [6] M. Rosenbaum, F. Zhao, M. Quaa, H. Wulff, U. Schröder, F. Scholz, Appl. Catal. B: Environ. 74 (2007) 262.
- [7] R. Fleischmann, H. Böhm, Electrochim. Acta 22 (1977) 1123.
- [8] P.N. Ross Jr., J. Macdonald, P. Stonehart, J. Electroanal. Chem. 63 (1975) 450.
- [9] B. Vidick, J. Lemaitre, B. Delmon, J. Catal. 99 (1986) 428.
- [10] S.T. Oyama, P. Clark, X. Wang, T. Shido, Y. Iwasawa, S. Hayashi, J.M. Ramallo-Lopez, F.G. Requejo, J. Phys. Chem. B 106 (2002) 1913.
- [11] E. Iglesia, F.H. Ribeiro, M. Boudart, J.E. Baumgartner, Catal. Today 15 (1992) 307.
- [12] R.B. Levy, M. Boudart, Science 181 (1973) 547.
- [13] P. Liu, J.A. Rodriguez, Catal. Lett. 91 (2003) 247.
- [14] L. Bennett, J.R. Cuthill, A. McAlister, N. Erickson, R. Watson, Science 184 (1974).
- [15] L. Bennett, J.R. Cuthill, A. McAlister, N. Erickson, R. Watson, Science 187 (1975) 858.
- [16] G.A. Tsirlina, O.A. Petrii, Electrochim. Acta 32 (1987) 637.
- [17] K.M. Andersson, L. Bergström, Int. J. Refractory Metals Hard Mater. 18 (2000) 121.
- [18] J.D. Voorhies, J. Electrochem. Chem. 219 (1972).
- [19] A.M. Human, H.E. Exner, Mater. Sci. Eng. A 209 (1996) 180.
- [20] B. Bozzini, G.P. De Gaudenzi, A. Fanigliulo, C. Mele, Mater. Corrosion 54 (2003) 295.
- [21] M.A. Zellner, G.C. Jingguang, Catal. Today 99 (2005) 299.
- [22] E.C. Weigert, A.L. Stottlemeyer, M.B. Zellner, G.C. Jingguang, J. Phys. Chem. C 111 (2007) 14617.
- [23] B. Bozzini, G.P. De Gaudenzi, A. Fanigliulo, C. Mele, Corrosion Sci. 453 (2004).
- [24] J.W. Johnson, C.L. Wu, Electrochem. Sci. 1909 (1971).
- [25] P.N. Ross, P. Stonehart, J. Catal. 39 (1975) 298.
- [26] R.D. Armstrong, J. Electrochem. Sci. 118 (1971) 568.
- [27] H. Böhm, Electrochim. Acta 15 (1970) 1273.
- [28] H. Binder, A. Köhling, W. Kuhn, G. Sandstede Angew. Chemie Int. Ed. 8 (1969) 757.
- [29] P. Zoltowski, Electrochim. Acta 31 (1986) 103.
- [30] P.R. Patil, S.H. Pawar, P.S. Patil, Solid State Ionics 136–137 (2000) 505.
- [31] K. von Bender, H. Binder, W. Faul, G. Sandstede, Chemie-Ing. Technol. 43 (1971) 1223.
- [32] M.H. Dhandehari, J. Electrochem. Sci. Technol. 127 (1980) 2144.
- [33] C. Ma, Y. Gan, Y. Chu, H. Huang, D. Chen, B. Zhou, T. Nonferr, Metal Soc. 14 (2004) 11.
- [34] H. Binder, A. Köhling, W. Kuhn, G. Sandstede, Angew. Chem. Int. Ed. 8 (1969) 757.
- [35] B. Ganesan, J.S. Lee, Angew. Chem. 117 (2005) 2.
- [36] H.H. Hwu, J.G. Chen, J. Phys. Chem. B 107 (2003) 2029.
- [37] H.H. Hwu, J.G. Chen, K. Kourtakis, J.G. Lavin, J. Phys. Chem. B 105 (2001) 10037.
- [38] H. Okamoto, G. Kawamura, A. Ishiwaka, T. Kudo, J. Electrochem. Soc. 134 (1987) 1645.
- [39] H.J. Zheng, C.N. Ma, J.G. Huang, G.H. Li, J. Mater. Sci. Technol. 21 (2005) 545.
- [40] P.N. Ross, P. Stonehart, J. Catal. 48 (1977) 42.
- [41] F. Scholz, U. Schröder, R. Gulaboski, Electrochemistry of Immobilized Particles and Droplets, Springer, Berlin, Heidelberg, New York, 2005.
- [42] G.T. Burstein, M.J. McInerney, A. Vossen, Electrochem. Solid-State Lett. 5 (2002) A80.